RSC Advances

ROYAL SOCIETY OF CHEMISTRY

www.rsc.org/advances

Journal Name

ARTICLE

Spatially-controlled Growth of Platinum on Gold Nanorods with Tailoring Plasmonic and Catalytic Properties†

Received 00th January 20xx,
Accepted 00th January 20xx

DOI: 10.1039/x0xx00000x

www.rsc.org/

Yun Rong,[‡a] Anirban Dandapat,[‡b] Youju Huang, *[a] Yoel Sasson,[b] Lei Zhang,[a] Liwei Dai,[a] Jiawei Zhang,[a] Zhiyong Guo [c] and Tao Chen*[a]

We have described the synthesis of bimetallic dendritic platinum decorated gold nanorods (AuNRs) by spatial control of Pt growth over gold nanorods via a heterogeneous seed-mediated growth method. The amounts of the Au seed and Pt-precursor were accustomed to achieve a tunable volume fraction of Pt coverage on the Au NRs surface. Pt nanostructures were spatially separated from each other, which was highly favorable for promising optical and catalytic properties. The dendritic-Pt decorated AuNRs with variable Au/Pt ratio were exploited to study their surface plasmonic properties and catalytic activities. Interestingly, Pt decorated AuNRs resemble strong surface plasmon resonance (SPR) peak due to noncompact dendritic Pt shell in contrast to the conventional core-shell Au@Pt nanoparticles (NPs). Moreover, the longitudinal peak of AuNRs was finely tuned from 820 to 950 nm (NIR region) by controlling the volume fraction of Pt decoration over the AuNRs. The catalytic activity of the dendritic-Pt decorated AuNRs was studied on the reduction of 4-nitrophenol (4-NP) by sodium borohydride ($NaBH_4$) as reducing agent and found to be superior to the activities compared to monometallic Au NRs. Considering practical application, dendritic-Pt decorated AuNRs nanostructures were successfully immobilized on the hydrophilic polyvinylidene difluoride (PVDF) film as an efficient reusable catalyst.

Introduction

An emerging bulk of research has been focused on noble metal-based nanostructures to be applied as high-performance catalysts in the fields ranging from chemical synthesis and energy conversion to environmental issues. It has been established that bimetallic nanocatalysts often display enhanced physical and chemical properties compared to those of their monometallic counterparts, as they provide more opportunities to optimize their activity by adjusting the charge transfer between the different metals, local coordination environment, and surface elemental distribution.[1-11] Among different metal compositions, Au-, Pd-containing bimetallic systems has been extensively studied.[4, 7, 12] Particularly，Pt based catalysts have been proven to be most efficient catalyst in various reactions.[10, 13-16] Therefore, considering very high cost of Pt, fabrication of Pt-based catalysts with high performance and as economic as possible is very urgent.

To this end, various Pt-based nanostructures have been synthesized and found bimetallic nanostructures are much active compared to only Pt nanoparticles (NPs) as catalyst.[14, 17] Combining another metal (e.g.,Ag[18], Pd,[19, 20] Au,[10, 21] Fe,[22] ,Cu[23] *etc*) with Pt not only give the benefit of improved bimetallic properties to enhance the catalytic performance, but also reduce the level of Pt loading to make the materials cheaper. In this direction, we aimed to combine the fascinating properties of Au nanorods (AuNRs),[24-27] such as its unique optical properties, excellent chemical and thermal stability, with the high catalytic activity of tiny Pt NPs.[28-31] However, most reported Au-Pt bimetallic NPs were either alloyed[32] or core-shell structure[33] and these alloyed or core-shell structure would dramatically inhibit plasmonic property of the Au-Pt bimetallic NPs.[34-37] Herein, we report an effective route to obtain Pt NPs decorated Au NRs by spatial control of Pt growth over Au NRs. Controlling the amounts of the AuNRs and the Pt-precursor, tunable volume fractions of AuNRs were decorated by Pt nanostructures to exploit their structure and composition dependent optical and catalytic properties. Interestingly, we observed strong surface plasmon resonance peak of the dendritic-Pt decorated AuNRs, which is in contrast to most of the previous reports where SPR of Au core was damped due to Pt deposition.[10, 34-37]. Since the Pt NPs are spatially separated from each other, is highly favourable for maximizing the Pt surface area to obtain high catalytic activities. We performed their catalytic activities towards 4-nitrophenol (4-NP) reduction and found superior activities

[a] *Division of Polymer and Composite Materials, Ningbo Institute of Material Technology and Engineering, Chinese Academy of Sciences, No. 1219 Zhongguan West Road, Zhenhai District, Ningbo 315201, China. E-mail: yjhuang@nimte.ac.cn and tao.chen@nimte.ac.cn.*
[b] *Casali Center of Applied Chemistry, Institute of Chemistry, the Hebrew University of Jerusalem, Jerusalem 91904, Israel.*
[c] *School of Materials Science and Chemical Engineering, Ningbo University, Ningbo 315211, PR China*
†Electronic Supplementary Information (ESI) available. See DOI: 10.1039/x0xx00000x
‡ These authors contribute equally to this work.

compared to monometallic Au NRs. For practical application, catalyst in the form of thin film is highly desirable due to their advanced benefits e.g. easy handling and insertion/removal from the reaction medium etc.[38, 39] In this aim, the dendritic-Pt decorated AuNRs were deposited on the hydrophilic polyvinylidene difluoride (PVDF) film. The nanocomposite films showed excellent catalytic performances and reused for several cycles with very less significant deterioration of their original activity.

Experimental

Materials

Hexadecyltrimethylammonium bromide (CTAB, ＞99.0%) was purchased from Sigma-Aldrich. Sodium citrate ($C_6H_5Na_3O_7 \cdot 2H_2O$, 99.0 %), sodium borohydride ($NaBH_4$, 99.0%), silver nitrate ($AgNO_3$, >99.0%), ascorbic acid (AA, 99.7%), hydrochloric acid (HCl, 37wt %. in water), sodium iodide (NaI, 99.0 %) were purchased from Sinopharm Chemical (Shanghai, China). Sodium oleate (NaOL, >97.0 %) was purchased from TCI. Hydrogen tetrachloroaurate trihydrate ($HAuCl_4 \cdot 3H_2O$, 99.99 %), platinum (II) chloride ($PtCl_2$, 99.0%), 4-nitrophenol (4-NP), Tris (hydroxymethyl) aminomethane (Tris), 3-hydroxytyramine hydrochloride (dopamine·HCl) was obtained from Aladdin Company in Shanghai. Other reagents and solvents were analytical reagent grade and were used as received from Sinopharm Chemical Reagent.

Synthesis of Gold NRs

The gold nanorods was prepared by a previously reported method.[40] The seed solution was prepared by rapidly injecting 0.6 mL of fresh 0.01 M $NaBH_4$ into the mixture of 5 mL of 0.5 mM $HAuCl_4$ and 5 mL of 0.2 M CTAB solution in a 20 mL scintillation vial under vigorous stirring (1200 rpm).The stirring was stopped after 2 min and the seed solution was aged at room temperature for 30 min before use. To prepare the growth solution, 3.5g of CTAB and 0.617g of NaOL were dissolved in 125 mL of warm water. 9 mL of 4 mM $AgNO_3$ solution and 125 mL of 1 mM $HAuCl_4$ solution were added when solution was cooled down to 30 °C. After 90 min of stirring (700 rpm), 0.75 mL of HCl (37 wt. % in water, 12.1 M) was introduced to adjust the pH. After another 15 min of slow stirring at 400 rpm, 0.625 mL of 0.064 M ascorbic acid (AA) was added and the solution was vigorously stirred for 30 s. Finally, 0.2 mL seed solution was injected into the growth solution. The resultant mixture was stirred for 30 s and left undisturbed at 30 °C for 12 hours for NRs growth. The resulting nanocrystals were washed twice by centrifugation prior to characterization and re-dispersed in water for further use.

Synthesis of dendritic-Pt decorated AuNRs

Pt decorated AuNRs were prepared by a seed-mediated method which was slightly different from the previous method[41] by changing the amount of seed solution and the reducing agent. In the presence of iodide ions (50 μM), 10 mL of 0.05 M CTAB, 5 mL of re-dispersed Au nanorods, 500 μL of 0.2 mM $AgNO_3$, and 500 μL of 0.1 M ascorbic acid were added to a vial. The mixture was kept at 70 °C. After 1 hour, 480 μL of 0.1 M HCl and, 110 μL of 2 mM aqueous H_2PtCl_6 solution were added to the mixture, which was then kept at 70 °C 4 hr. After this reaction, the sample was centrifuged at 7000 rpm and re-dispersed in DI water. For other different volume fractions dendritic platinum coated AuNRs，the aqueous H_2PtCl_6 solution added were 55, 220 and 440 μL.

Catalytic reduction of nitrophenol (4-NP)

The catalytic reduction of 4-NP was monitored on a TU-1810 spectrophotometer UV-vis spectrophotometer in the range of 200–600 nm at room temperature. An aqueous solution of 20 μL of 10 mM 4-NP solution and 2.5 mL water were added to 0.1 ml of 0.1 M freshly prepared $NaBH_4$ solution. Then, 0.5 mL of nanoparticle solution was added and thoroughly mixed. Each catalytic experiment was performed at least 3 times to ensure the reproducibility. To prepare the dendritic-Pt decorated AuNRs loaded reusable composite film, 20 mL of dendritic-Pt decorated AuNRs synthesized with 440 μL aqueous H_2PtCl_6 solution was added into 20 mL aqueous solution which contained 2 mg/mL dopamine and 10 mM Tris buffer solution, then the PVDF film was immersed in the solution for 4 days at room temperature. PVDF membrane was prepared by the previous reported method.[42] The dendritic-Pt decorated AuNRs loaded PVDF film was washed with running water three times and dried in air. For the recycle catalytic performance of the dendritic-Pt decorated AuNRs loaded PVDF film, the film was cut into a 1 cm×4 cm piece then immersed into an aqueous solution of 20 μL of 10 mM 4-NP solution，2.5 mL of water and 0.1 mL of 0.1 M freshly prepared $NaBH_4$ solution for 2 hour. The film was washed with running water three times and dries in air for next catalytic performance test. The experiment was repeated 7 times.

Characterization

Ultraviolet-visible (UV-vis) absorption spectra were recorded with TU-1810 spectrophotometer from Beijing Purkinje General Instrument Co. Ltd. in transmission mode. Transmission electron microscopy (TEM) was performed on a JEOL JEM-2100F instrument and operated at 200 kV. Scanning electronic microscopy (SEM) measurements were carried out by a JEOL JMS-6700F scanning microscope.

Results and Discussion

Heterogeneous seed-mediated growth route was introduced to produce bimetallic dendritic-Pt decorated AuNRs, as illustrated schematically in Fig.1a. The nanostructures were characterized by UV-visible spectra and TEM investigations. Au NRs (aspect ratio ~3; Fig. S1) were first synthesized in an aqueous solution employing a binary mixture of surfactant, namely CTAB and NaOL.[40] Next, dendritic-Pt decorated AuNRs were prepared via heterogeneous seed-mediated growth of Pt nanostructures over the Au NR seeds by reducing H_2PtCl_6 with ascorbic acid under the assistance of CTAB, iodide ions and Ag^+ ions. As revealed by HR-TEM images (Fig. 1b) and elemental mapping (Fig. 1c, d), the dendritic Pt shell is composed of many small Pt nanostructures with the size of ~ 4-5 nm. The Pt growth on the Au NRs was spatially controlled to achieve different volume fraction of Pt-nanostructure coverage over the Au NRs (ESI; Fig. S2) by controlling the amounts of Pt-precursor i.e. H_2PtCl_6 in a fixed amount of Au NRs seed. First, Pt

nanostructures were selectively deposited at the tips of Au NRs

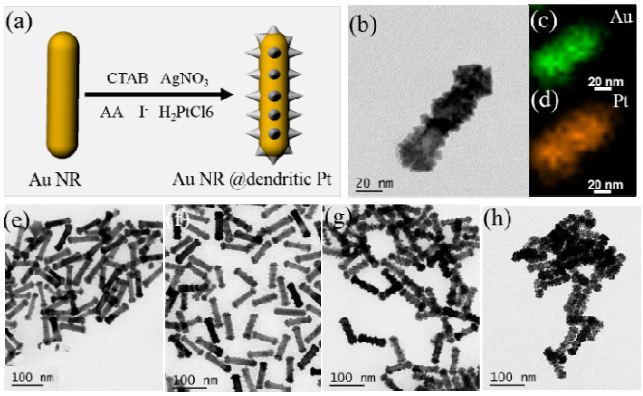

Fig. 1. (a) Scheme of the synthesis of dendritic-Pt decorated AuNRs; (b) TEM images of dendritic-Pt decorated AuNRs. (c) and (d) show the elemental mappings of one dendritic-Pt decorated AuNRs. The green and orange colours in the elemental maps stand for gold and platinum, respectively; TEM images (e-h) of nanostructures with varying volume fractions dendritic platinum obtained by adding different amounts of 2 mM H_2PtCl_6 solution: (e) 55μL, (f) 110μL, (g) 220μL and (h) 440μL, respectively.

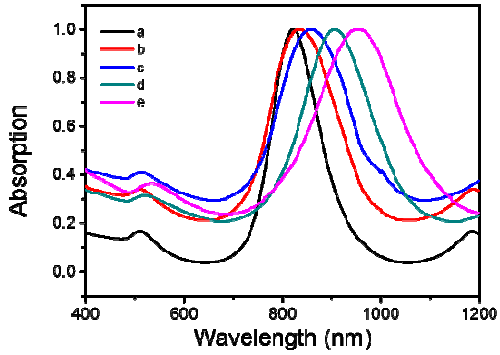

Fig. 2. UV-vis absorption spectra of (a)Au NR and (b-e) Au NR decorated with dendritic platinum synthesized with different amount of 2 mM H_2PtCl_6 solution（55 μL in a，110 μL in b, 220 μL in c and 440 μL in d, respectively.）

(Fig. 1e & Fig. S3a) in the presence of iodide ions and Ag^+. In presence of Ag^+ and iodide ions, Pt would be selectively deposited at the edges or tips (of the AuNRs), where surface energy is higher and co-ordination number is lower.[41] Higher surface energy and lower cordination number generates more reactive sites at the tips, and thus Pt prefers to be deposited on the tips of the NRs.[41] With increasing the amounts of H_2PtCl_6 (2 mM) solution from 55 μL to 440 μL, as shown by the TEM images (Fig.1e-h and Fig. S3), tips of the Au NRs was first covered by tiny Pt NPs (Fig. 1e) followed by the deposition on the side faces, finally forming dendritic discontinuous Pt-shell over the Au NRs (Fig. 1h). Much higher amounts of H_2PtCl_6 solution (5ml; 2mM) produced core-shell AuNR@Pt nanostructures (ESI; Fig. S4). These dendritic-Pt decorated AuNRs were highly monodispersed as revealed by their TEM (Fig.1) and SEM (ESI; Fig. S5) images. Due to this unique dendritic structure, both Au and Pt surfaces remain highly accessible by the reactants which will make the nanostructures efficient for catalytic applications.

Optical properties of Au and dendritic-Pt decorated AuNRs were characterized by UV-Vis absorption spectra. Fig.2 shows the UV-Vis absorption spectra of the as-prepared Au NRs (a) and the dendritic-Pt decorated AuNRs (b-e). As can be seen from the Fig.2, Au NRs display two characteristic absorption peaks at 515 and 820 nm, corresponding to a weak transverse surface plasmon (TSP) resonance and a strong longitudinal surface plasmon (LSP) resonance, respectively. Interestingly, we observed a gradual red-shifting of the longitudinal peak with fine tuning from 820 nm to 950 nm by controlling the amounts of 2mM H_2PtCl_6 (55 μL to 440 μL), while the transverse resonance wavelength was slightly shifted or remains unchanged (ESI; Fig. S6). Much higher shifting of longitudinal peak results from the higher polarizability of the NRs at the longitudinal plasmon resonance than at the transverse plasmon resonance.[43] The red-shifting can be correlated to the discontinuous dendritic growth of Pt shell similar to the case of Au@Pd system.[44] In a previous report, Chen et al[44] established that a discontinuous Pd shell on Au NR causes red-shifting, whereas continuous Pd shell gave blue-shifting of the SPR of Au NR core. In a similar way, we have been able to tune the longitudinal peak of Au-NR@dendritic-Pt nanostructures from 820 nm to 950 nm (NIR region) by controlling the fraction of Pt coverage over the AuNR's surface. This tunable localized surface plasmon resonance wavelength towards NIR region is very much useful for different biomedical applications as well as for some in situ spectroscopic characterization of catalytic reactions.

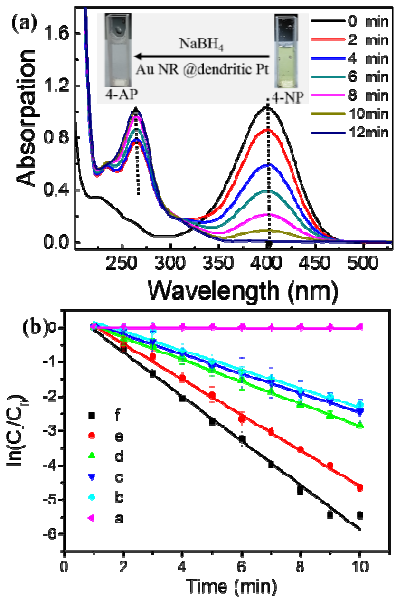

Fig.3. (a) Time-dependent UV-vis absorption spectra of 4-NP reduced by $NaBH_4$ and catalyzed by dendritic-Pt decorated AuNRs. (b) Plot of ln (C_t/C_0) as a function of time of different catalyst (a, no catalyst; b, Au NR; c-f, dendritic-Pt decorated AuNRs synthesized with different amount of 2mM H_2PtCl_6

solution (55 µL in c， 110 µL in d, 220 µL in e and 440 µL in f, respectively)).

This interesting dendritic morphology of the nanostructures with varying Au/Pt composition ratio motivated us to explore the catalytic activity of the nanostructures. The reduction of 4-NP by $NaBH_4$ in aqueous solution is well known and easily monitored reaction, and thus chosen as a model reaction here to test the catalytic activities of the developed materials.[45] The reaction was monitored by collecting UV-visible absorption spectrum of the mixture of 4-NP and $NaBH_4$ at different time. Initially the solution showed absorption maxima at ~400 nm due to the formation of 4-nitrophenolate ion in alkaline solution which is caused by the addition of $NaBH_4$ solutions. This absorption spectrum remains almost unaltered with time in absence of any catalyst, which suggests that the reduction did not proceed. In the contrary, presence of very small amounts of Au-Pt nanostructures causes reduction of 4-NP very rapidly as observed in their time-dependent UV-visible absorption spectra (Fig.3a).

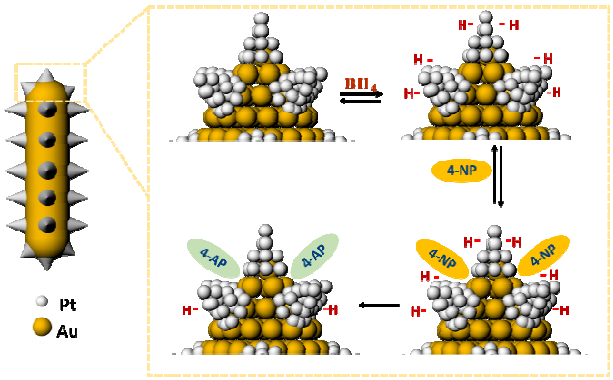

Fig.4. A schematic representation for the possible mechanism of 4-NP reduction on dendritic-Pt decorated AuNR's surface.

In addition to the successive decrease in the absorption peak at 400 nm, a new peak at 280 nm was gradually developed due to the reduction of 4-NP to 4-aminophenol (4-AP). We performed the catalytic activities of all the different nanostructures and a representative study using dendritic-Pt decorated AuNRs (Fig.1h; nanostructures synthesized by using 440 µL of H_2PtCl_6 solution) as catalyst is presented in Fig.3a. Rate constants were calculated by plotting ln (C_t/C_0) (where C_0 and C_t are the concentrations of 4-AP at time zero and t, respectively) as a function of time for all the structures and have been presented in Fig.3b and table S1. It is observed that the activity was gradually increased with increasing the loading of Pt. However, fully covered AuNR@Pt core-shell nanostructures showed lower activity compared to dendritic-Pt decorated AuNRs obtained by adding 440 µL of 2mM H_2PtCl_6 solution (ESI; Fig. S7). The result is consistent with a previous report by Zheng et al.,[46] where an improved catalytic activity was observed by Pd-tipped Au NRs than that of the core-shell AuNR@Pd nanostructures towards 4-NP reduction. The enhanced catalytic activities of the Pd-tipped AuNRs were attributed to the hot electrons transfer from Au to Pd. The interfacial interaction between two different metal segments is essential for the improved catalysis. In a similar way, our developed dendritic-Pt decorated AuNRs with simultaneous exposure of Pt and Au surfaces result in the improved catalytic activity over the core-shell nanostructure.

It is widely accepted that the catalytic reduction of 4-NP by any metal NPs catalyst involved the adsorption of both BH_4^- and 4-NP from aqueous solution on the surface of the NPs, and then electron/hydride transfer from BH_4^- to 4-NP to produce 4-AP.[17, 45] Notably, 4-NP prefers to adsorb on Au while BH_4^- is more likely to adsorb on Pt.[17] Thereby, the mechanism for the reduction of 4-NP by $NaBH_4$ in presence of the developed bimetallic dendritic-Pt decorated AuNRs could be proposed as illustrated in Fig.4. Firstly, 4-nitrophenolate and BH_4^- ions are adsorbed on the neighboring Au and Pt sites, respectively at the surface of dendritic-Pt decorated AuNRs. BH_4^- produces transient metal hydrides with Pt atoms and then the adsorbed hydrogens were transferred to 4-nitrophenolate ion adsorbed adjacent Au sites and reduced it to 4-AP. Due to this synergistic effect of Au and Pt, bimetallic dendritic-Pt decorated AuNRs showed better catalytic activity than that of Au NRs.

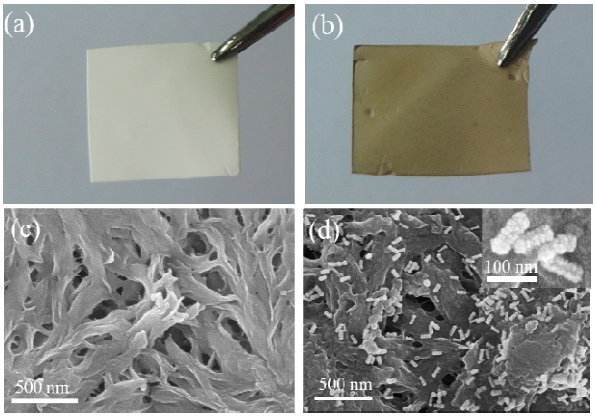

Fig.5. Photograph (a, b) and SEM images (c, d) of PVDF film before (a, c) and after (b, d) the deposition of dendritic-Pt decorated AuNRs.

In a successful catalytic reaction, reusability of the catalyst is very important. In this aim, we developed a composite film, where dendritic-Pt decorated AuNRs were deposited on PVDF film by the mussel inspired polymer polydopamine (PDA). PDA can be easily deposited on virtually all types of inorganic and organic substrates.[47] Very recently, PDA has been applied in various catalytic systems and served as a catalyst carrier due to its unique merits.[48] The colour of the PVDF film was changed from white to black-brown (Fig.5a and 5b), indicating the successful deposition of dendritic-Pt decorated AuNRs on the PVDF film. To further confirm the deposition of the AuNRs@dendritic-Pt on the PVDF film, the morphology of the PVDF film before and after the deposition of dendritic platinum decorated Au NRs were analysed by SEM. The PVDF film has a porous multilayer structure (Fig.5c) with unique properties of high specific surface area and chemical stability, which is an ideal candidate as catalyst carrier. The

AuNRs@dendritic-Pt nanostructures were immobilized and randomly dispread on the PVDF film (Fig.5d).

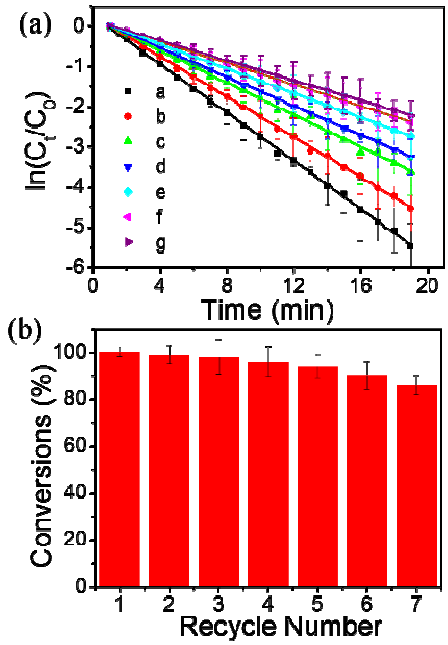

Fig.6.The plot of ln (C_t/C_0) as a function of time of 4-NP and (b) Conversion efficiency of 4-NP in 2 hours reaction in 7 successive cycles by using Au-NR@dendritic-Pt on the PVDF film as catalyst (a-g represent the recycle 1-7 respectively).

The catalytic property of this nanocomposite film was tested in 7 consecutive cycles (Fig.6a). After each cycle, the catalyst film was directly withdrawn from the reaction solution, washed with water, and allowed to perform the next cycle. As revealed in Fig.6b, almost identical catalytic activities were observed. Almost 90% conversion was measured even at the 7th cycle, indicating the excellent stability and recyclability of the catalytic films. The dendritic-Pt decorated AuNRs deposited PVDF film also possessed the property of oil/water separation[42] (oil/water separation result was shown in Fig. S 8), which would provide new opportunities to develop bifunctional membrane with both catalytic property and oil/water separation

Conclusions

In conclusion, we reported the synthesis of dendritic-Pt decorated AuNRs by spatially controlled Pt growth over the Au NRs in a facile wet chemical method and the synthesized hybrid bimetallic nanostructures exhibit tunable localized surface plasmon resonance from visible to NIR region and excellent catalytic activity. We have demonstrated that catalysis and optical properties of the hybrid nanostructures can be readily tailored by adjusting the surface decoration density of Pt NPs on the surfaces of Au NRs. Pt NPs remained spatially separated from each other, which is highly favourable for maximizing the Pt surface area to obtain very high catalytic activities. For successful catalytic application, the nanostructures were loaded in a solid PVDF film support and the composite film was used as efficient catalyst maintaining excellent stability and reusability. Apart from catalytic activities, considering their very interesting optical properties, these unique materials demands to be applied in various biomedical applications.

Acknowledgements

We thank the Chinese Academy of Science for Hundred Talents Program, Chinese Central Government for Thousand Young Talents Program, the Natural Science Foundation of China (21404110, 51473179, 81273130 and 51573203), Ningbo Science and Technology Bureau (Grant 2014B82010 and 2015C110031), the Technology Foundation for Selected Overseas Chinese Scholar, and Ministry of Personnel of China (2015).

References

1. X. Peng, Q. Pan and G. L. Rempel, *Chem. Soc. Rev.*, 2008, **37**, 1619-1628.
2. M. T. Reetz, M. Winter, G. Dumpich, J. Lohau and S. Friedrichowski, *J. Am. Chem. Soc.*, 1997, **119**, 4539-4540.
3. L. Zhu, L. Zheng, K. Du, H. Fu, Y. Li, G. You and B. H. Chen, *RSC Adv.*, 2013, **3**, 713-719.
4. D. Jana, A. Dandapat and G. De, *J. Phys. Chem. C*, 2009, **113**, 9101-9107.
5. N. Sharma, H. Ojha, A. Bharadwaj, D. P. Pathak and R. K. Sharma, *RSC Adv.*, 2015, **5**, 53381-53403.
6. L. Kuai, X. Yu, S. Wang, Y. Sang and B. Geng, *Langmuir*, 2012, **28**, 7168-7173.
7. R. Su, R. Tiruvalam, A. J. Logsdail, Q. He, C. A. Downing, M. T. Jensen, N. Dimitratos, L. Kesavan, P. P. Wells, R. Bechstein, H. H. Jensen, S. Wendt, C. R. A. Catlow, C. J. Kiely, G. J. Hutchings and F. Besenbacher, *ACS Nano*, 2014, **8**, 3490-3497.
8. A. Mattiuzzi, I. Jabin, C. Mangeney, C. Roux, O. Reinaud, L. Santos, J.-F. Bergamini, P. Hapiot and C. Lagrost, *Nature Communications*, 2012, **3**.
9. S. Guo, J. Li, S. Dong and E. Wang, *J. Phys. Chem. C*, 2010, **114**, 15337-15342.
10. H. Ataee-Esfahani, L. Wang, Y. Nemoto and Y. Yamauchi, *Chem. Mater.*, 2010, **22**, 6310-6318.
11. Y. Huang, P. Kannan, L. Zhang, T. Chen and D.-H. Kim, *RSC Adv.*, 2015, **5**, 58478-58484.
12. O. V. Belousov, N. V. Belousova, A. V. Sirotina, L. A. Solovyov, A. M. Zhyzhaev, S. M. Zharkov and Y. L. Mikhlin, *Langmuir*, 2011, **27**, 11697-11703.
13. T.-D. P.-o.-A. Bimetallic, *J. Phys. Chem. C*, 2010, **114**, 15337-15342.
14. B. Lim, M. Jiang, P. H. C. Camargo, E. C. Cho, J. Tao, X. Lu, Y. Zhu and Y. Xia, *Science*, 2009, **324**, 1302-1305.
15. C. Q. Wang, F. F. Ren, C. Y. Zhai, K. Zhang, B. B. Yang, D. A. Bin, H. W. Wang, P. Yang and Y. K. Du, *RSC Adv.*, 2014, **4**, 57600-57607.
16. Y.-W. Lee, A. R. Ko, D.-Y. Kim, S.-B. Han and K.-W. Park, *RSC Adv.*, 2012, **2**, 1119-1125.
17. C. Chu and Z. Su, *Langmuir*, 2014, **30**, 15345-15350.

18. Y. Huang, P. Kannan, L. Zhang, Y. Rong, L. Dai, R. Huang and T. Chen, *RSC Advances*, 2015, **5**, 94849-94854.
19. Y. Huang, A. R. Ferhan, A. Dandapat, C. S. Yoon, J. E. Song, E. C. Cho and D.-H. Kim, *J. Phys. Chem. C*, 2015, **119**, 26164-26170.
20. J. Zhang, Y. Mo, M. B. Vukmirovic, R. Klie, K. Sasaki and R. R. Adzic, *J. Phys. Chem. B*, 2004, **108**, 10955-10964.
21. Y. Jin and S. Dong, *J. Phys. Chem. B*, 2003, **107**, 12902-12905.
22. S. Guo and S. Sun, *J. Am. Chem. Soc.*, 2012, **134**, 2492-2495.
23. S. Zhou, B. Varughese, B. Eichhorn, G. Jackson and K. McIlwrath, *Angew. Chem., Int. Ed.*, 2005, **117**, 4615-4619.
24. Y. Huang, A. R. Ferhan and D.-H. Kim, *Nanoscale*, 2013, **5**, 7772-7775.
25. Y. Huang and D.-H. Kim, *Nanoscale*, 2011, **3**, 3228-3232.
26. Y. Huang, L. Wu, X. Chen, P. Bai and D.-H. Kim, *Chem. Mater.*, 2013, **25**, 2470-2475.
27. T. Xie, C. Jing, W. Ma, Z. Ding, A. J. Gross and Y.-T. Long, *Nanoscale*, 2015, **7**, 511-517.
28. A. Dandapat, D. Jana and G. De, *ACS Appl. Mater. Interfaces*, 2009, **1**, 833-840.
29. B. Sheng, L. Hu, T. Yu, X. Cao and H. Gu, *RSC Adv.*, 2012, **2**, 5520-5523.
30. C. Zhang, Y. Zhou, Y. Zhang, Q. Wang and Y. Xu, *RSC Adv.*, 2015, **5**, 12472-12479.
31. A. Dandapat, A. Mitra, P. K. Gautam and G. De, *Nanomater. Nanotechnol.*, 2013, **3**, 11.
32. Y.-C. Lu, Z. Xu, H. A. Gasteiger, S. Chen, K. Hamad-Schifferli and Y. Shao-Horn, *J. Am. Chem. Soc.*, 2010, **132**, 12170-12171.
33. K.-J. Chen, W.-N. Su, C.-J. Pan, S.-Y. Cheng, J. Rick, S.-H. Wang, C.-C. Liu, C.-C. Chang, Y.-W. Yang and C.-H. Wang, *J. Mater. Chem. B*, 2013, **1**, 5925-5932.
34. G. De and C. N. R. Rao, *J. Mater. Chem. C*, 2005, **15**, 891-894.
35. H.-D. Koh, S. Park and T. P. Russell, *ACS Nano*, 2010, **4**, 1124-1130.
36. M. Cheng, M. Zhu, Y. Du and P. Yang, *Inter. J. Hydro. Energy*, 2013, **38**, 8631-8638.
37. Z. Y. Bao, D. Y. Lei, R. Jiang, X. Liu, J. Dai, J. Wang, H. L. W. Chan and Y. H. Tsang, *Nanoscale*, 2014, **6**, 9063-9070.
38. A. Dandapat and G. De, *J. Mater. Chem.*, 2010, **20**, 3890-3894.
39. H. Gnayem, A. Dandapat and Y. Sasson, *Chem. Euro. J.*, 2015, DOI: 10.1002/chem.201503900.
40. X. Ye, C. Zheng, J. Chen, Y. Gao and C. B. Murray, *Nano Lett.*, 2013, **13**, 765-771.
41. S. Ham, H. J. Jang, Y. Song, K. L. Shuford and S. Park, *Angew. Chem.*, 2015, **127**, 9153-9156.
42. M. Tao, L. Xue, F. Liu and L. Jiang, *Adv. Matter.*, 2014, **26**, 2943-2948.
43. H. Chen, L. Shao, Q. Li and J. Wang, *Chem. Soc. Rev.*, 2013, **42**, 2679-2724.
44. H. Chen, F. Wang, K. Li, K. C. Woo, J. Wang, Q. Li, L.-D. Sun, X. Zhang, H.-Q. Lin and C.-H. Yan, *ACS Nano*, 2012, **6**, 7162-7171.
45. S. Wunder, F. Polzer, Y. Lu, Y. Mei and M. Ballauff, *J. Phys. Chem. C*, 2010, **114**, 8814-8820.
46. Z. Zheng, T. Tachikawa and T. Majima, *J. Am. Chem. Soc.*, 2015, **137**, 948-957.
47. Y. Liu, K. Ai and L. Lu, *Chem. Rev.*, 2014, **114**, 5057-5115.
48. A. Ma, Y. Xie, J. Xu, H. Zeng and H. Xu, *Chem. Commun.*, 2015, **51**, 1469-1471.

Table of Content Entry

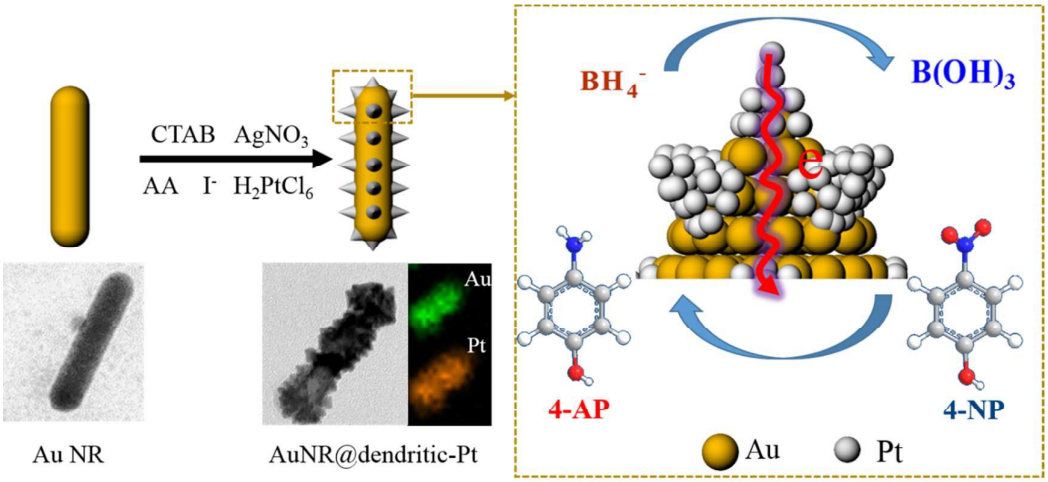

A dendritic platinum decorated gold nanorods with tailoring optical and catalytic properties was synthesized by spatial control of Pt growth over gold nanorods.